

Altering the Regioselectivity of a Nitroreductase in the Synthesis of Arylhydroxylamines by Structure-Based Engineering

Jing Bai,^[a] Yong Zhou,^[b] Qi Chen,^[a] Qing Yang,^[a] and Jun Yang^{*[a]}

Nitroreductases have great potential for the highly efficient reduction of aryl nitro compounds to arylhydroxylamines. However, regioselective reduction of the desired nitro group in polynitroarenes is still a challenge. Here, we describe the structure-based engineering of *Escherichia coli* nitroreductase NfsB to alter its regioselectivity, in order to achieve reduction of a target nitro group. When 2,4-dinitrotoluene was used as the substrate, the wild-type enzyme regioselectively reduced the

4-NO₂ group, but the T41L/N71S/F124W mutant primarily reduced the 2-NO₂ group, without loss of activity. The crystal structure of T41L/N71S/F124W and docking experiments indicated that the regioselectivity change (from 4-NO₂ to 2-NO₂) might result from the increased hydrophobicity of residues 41 and 124 (proximal to FMN) and conformational changes in residues 70 and 124.

Introduction

Arylhydroxylamines are important intermediates in the synthesis of pharmaceuticals^[1] and fine chemicals.^[2] They are primarily prepared through reduction of aryl nitro compounds, and various methods have been developed to accomplish this transformation, including metal-mediated reduction,^[3] catalytic hydrogenation reduction using immobilized Pt catalysts^[4] or doped Pd catalysts,^[5] and biocatalytic reduction using baker's yeast,^[6] plant cells,^[7] or bacterial nitroreductases.^[8] These processes can chemoselectively reduce mononitro compounds bearing other substituent groups, and achieve the direct conversion of aryl nitro compounds into their corresponding arylhydroxylamines. However, regioselective reduction of a nitro group at an arbitrarily selected site in the case of dinitro or polynitro compounds is still a challenge.

Nitroreductases catalyze the NAD(P)H-dependent reduction of nitro groups to hydroxylamino groups using FMN as prosthetic group, in many cases with high regioselectivity. Bacterial nitroreductases show different regioselectivities toward the prodrug CB1954 (5-(aziridin-1-yl)-2,4-dinitrobenzamide). NfsA from *Escherichia coli* selectively reduces the 2-NO₂ group rather than the 4-NO₂ group,^[9] whereas NfsB reduces the 2-NO₂ and 4-NO₂ groups equally,^[10] NemA and AzoR from *E. coli*,^[11] YwrO from *Bacillus amyloliquefaciens*,^[12] and Yfk0 from *Bacillus licheniformis*^[13] show a preference for the 4-NO₂ group. For 2,4-di-

nitrobenzoate (another dinitroarene), PnbA reductase from *Lactobacillus plantarum* strain WCFS1 selectively reduces the 4-NO₂ group.^[14] Because of their high regioselectivity toward polynitro and/or dinitro compounds, nitroreductases are potential catalysts for regioselective synthesis of target hydroxylamines.

However, the native regioselectivity of a nitroreductase toward a particular dinitroarene might not satisfy the requirements of industrial or clinical applications. Protein engineering has been used to alter the regioselectivity of nitroreductases. The preferences of two mutants of *E. coli* nitroreductase NfsB (T41L and T41L/N71S, obtained by random mutagenesis) for the more cytotoxic 4-hydroxylamine derivative of CB1954 were shown to be greater than that of the wild-type enzyme.^[15,16] Although the crystal structures of the single mutants T41L and N71S were determined,^[16] the effects of these two mutations on regioselectivity were unclear, as were the effects of other residues. Biochemical analysis of enzyme regioselectivity toward various substrates might enable comparative studies to be performed, thereby resulting in a better understanding of the influences of different substituent groups on regioselectivity. However, current research is mainly focused on the regioselective activation of CB1954; nitroreductase regioselectivity against other dinitroarenes have not been widely reported. It would therefore be useful to investigate this further, in order to achieve the rational design of mutant enzymes with ideal regioselectivity.

The aim of this study was to investigate the effects of key nitroreductase residues and substrate substituents on enzyme regioselectivity. *E. coli* NfsB was chosen as the enzyme for mutagenic alteration, because it has been well characterized and crystal structures in both the ligand-bound^[10,17] and unbound^[18] forms have been determined. 2,4-Dinitrotoluene (24DNT) and 2,4-dinitroanisole (24DNAN) were selected so as to examine the possible effects of substituent groups on regio-

[a] Dr. J. Bai, Dr. Q. Chen, Prof. Dr. Q. Yang, Dr. J. Yang
School of Life Science and Biotechnology
Dalian University of Technology
No. 2 Linggong Road, Dalian-116023 (China)
E-mail: junyang@dut.edu.cn

[b] Dr. Y. Zhou
School of Software Technology, Dalian University of Technology
321 Tuqiang Street, Development Zone, Dalian (China)

Supporting information for this article is available on the WWW under <http://dx.doi.org/10.1002/cbic.201500070>.

selectivity. The best mutant successfully altered the native regioselectivity of NfsB toward these two substrates, and did not exhibit any activity loss. Based on site-directed mutagenesis, structural analysis, and molecular-docking experiments, the molecular basis of regioselective reduction of the nitroreductase NfsB is proposed. This might provide guidance for the design of desired regioselective catalysts in the future.

Results and Discussion

Analysis of regioselectivity of nitroreductase NfsB toward 2,4-dinitrotoluene

E. coli NfsB has been shown to be active toward a variety of nitro substrates.^[19] The reductive products of 24DNT generated by purified NfsB were identified by analyzing the metabolites by HPLC and mass spectrometry.

After anaerobic incubation for 30 min with nitroreductase NfsB, the substrate 24DNT ($t_R = 25.4$ min) disappeared, and a major product was detected ($t_R = 13.9$ min; Figure 1A). The molecular mass of the product was 168 Da, and it was identified as the monohydroxylamine, thus suggesting that NfsB reduced only one nitro group of 24DNT to generate the hydroxylamine; no other amine products were observed (Figure 1B). To further investigate the nitroreduction regioselectivity, we identified the position of the nitro group that was reduced, by converting the product to the corresponding amine. The products of 24DNT reduction were converted almost exclusively to 4-amino-2-nitrotoluene (4ANT; Figure 1C), with only a very

small peak corresponding to 2-amino-4-nitrotoluene (2ANT), thus indicating that purified NfsB regioselectively reduced the 4-NO₂ group of 24DNT.

Alteration of regioselectivity by site-directed mutagenesis

It is of interest to explore nitroreductases with different regioselectivity, capable of producing different hydroxylamine isomers, some of which could potentially be used as precursors of pharmaceuticals, pesticides, and dyes. Therefore, we tried to evolve mutant enzyme(s) for regioselective reduction of the 2-NO₂ group.

Based on the crystal structures of NfsB,^[10,17,18] four residues were chosen for mutagenesis: T41, N71, F70, and F124. Residues 41 and 71 were selected because they are inside the active pocket and their mutations were shown to alter the regioselectivity of NfsB against CB1954.^[15,16] Eight diverse mutants were constructed (T41V, T41I, T41L, T41F, N71T, N71S, N71Q, and N71L), and their effects on 24DNT reduction were investigated. F70 and F124 were previously thought to be related to the catalytic activity;^[20] they are located at the entrance to the active site, and thus might mediate regioselectivity by controlling substrate access to the pocket. They were therefore mutated to Ala, Asn, and Trp (small, polar, and aromatic residues, respectively). Activity and regioselectivity against 24DNT were determined by HPLC.

Substitutions at residue 41 resulted in clear changes to the preference for the 2- and 4-NO₂ groups of 24DNT (Figure 2). T41V and T41I mutants catalyzed reduction of 2-NO₂ to a lesser extent, whereas T41L and T41F shifted the selectivity from exclusively 4-NO₂ to both groups equally. The N71 and F124 mutants showed only slightly modified regioselectivity; no change was observed for F70 mutants (Figure S1 in the Supporting Information). These results suggest that hydrophobicity of the side chain at position 41 is a determinant of NfsB regioselectivity (change increasing with increasing hydrophobicity).

In order to investigate additive and/or synergistic effects of multiple residues,^[21] double mutants were constructed based on mutations that yielded improvements in the desired regioselectivity (T41L, T41F, N71S, F124N, and F124W). Apart from T41L/F124N, all mutants showed improved regioselectivity for 2-NO₂ over the corresponding single mutants (Figure S1). T41L/N71S was highly active and regioselective toward CB1954,^[15] but was

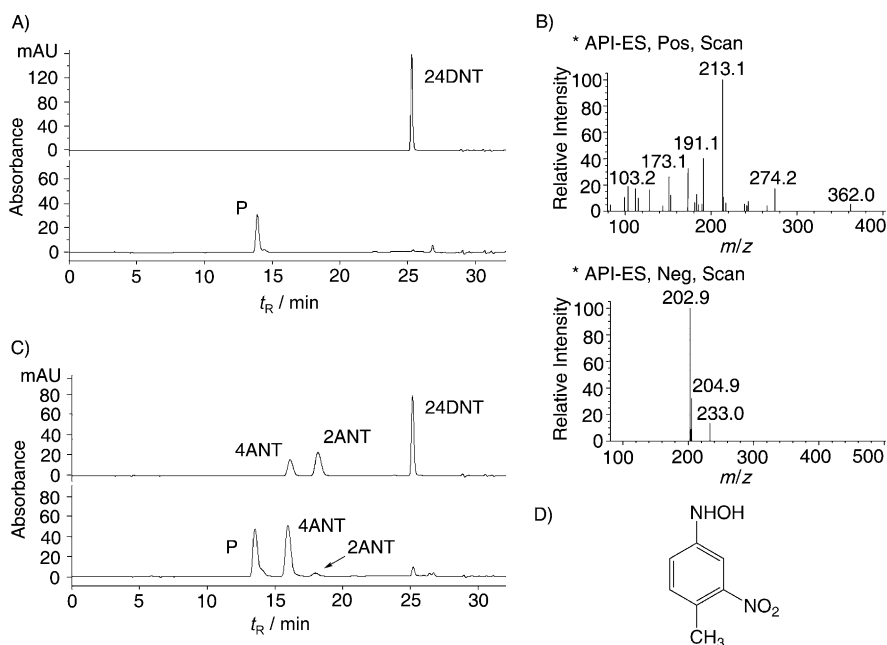


Figure 1. HPLC and MS analyses of products of 24DNT reduction by purified NfsB. A) HPLC profile after incubation for 30 min (lower trace) compared with control (no enzyme, upper trace). B) MS spectra of the reduced product (P) of 24DNT. The ions at m/z 191.1 and m/z 213.1 (positive mode) are the adducts $[M+Na]^+$ and $[M-H+2Na]^+$, respectively. The ion at m/z 202.9 (negative mode) is the adduct $[M < M + > Cl]^-$. Therefore, the molecular mass of the product was 168 Da. C) HPLC profile of the conversion product of peak P (lower trace) compared with that of authentic standard of amine derivative (upper trace). D) Structure of reduced product (P) of 24DNT.

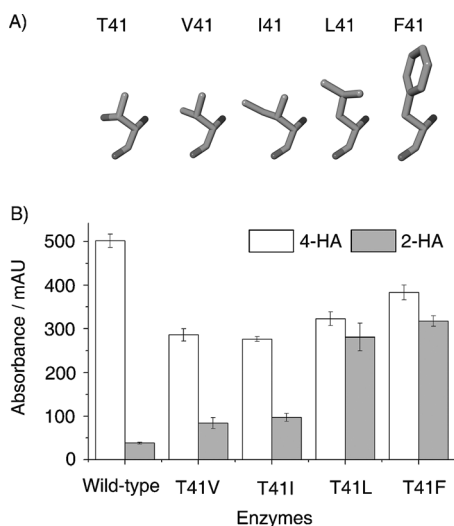


Figure 2. Effects of side-chain variation at residue 41 on regioselectivity. A) Side-chains at residue 41 of NfsB. B) Amounts of 2- or 4-hydroxylamine products of 24DNT reduction catalyzed by wild-type NfsB and the T41 mutants. The hydroxylamines were analyzed by HPLC (UV detection at 254 nm).

unable to produce 2-hydroxylamine from 24DNT regioselectively (Figure 3B).

Notably, although F124W (single mutant) was less beneficial for altering regioselectivity, F124W/T41L and F124W/N71S displayed a preference for the 2-NO₂ group of 24DNT, similarly to T41L/N71S. Substitution to a larger aromatic residue at position 124 (T41L/F124N and T41L/F124W) favored 2-hydroxylamine production, probably because of stronger hydrophobic and/or π -stacking interactions. Residue 124 was therefore a candidate for altering the enzyme regioselectivity, based on

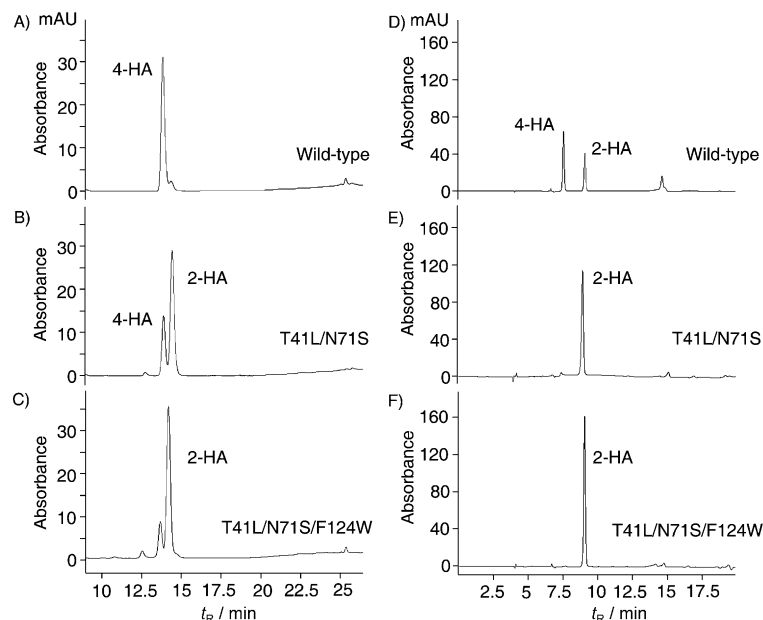


Figure 3. HPLC analysis of products of left: 24DNT and right: 24DNAN reduction catalyzed by wild-type NfsB, T41L/N71S, and T41L/N71S/F124W. Peaks corresponding to 2-hydroxylamine and 4-hydroxylamine products and substrates (24DNT and 24DNAN) are indicated.

possible synergistic effects with residues 41 and 71. The triple mutant T41L/N71S/F124W reduced the 2-NO₂ group to obtain 2-hydroxylamine as the major product (Figure 3C), thus demonstrating that the combination of the single-site mutation with the double mutation T41L/N71S further improved the desired regioselectivity.

Effects of substituent groups on regioselectivity of nitro-reductase NfsB

Wild-type NfsB displays different regioselectivity toward 24DNT and CB1954,^[10] thus implying that substrate substituents also affect regioselectivity. Mutagenesis studies showed that increasing the hydrophobicity of residue 41 changes enzyme substrate preference, thereby enabling it to reduce the 2-NO₂ group of 24DNT, probably by anchoring and stabilizing the 1-methyl group within the active pocket so that its adjacent nitro group is settled above N5 of FMN. The difference in hydrophobicity between the methyl and aziridiny groups might therefore lead to different regioselectivity.

To test this hypothesis, the substrate 24DNAN (containing the larger methoxy group adjacent to the 2-NO₂ group) was reduced by NfsB and selected mutants. Wild-type NfsB reduced either 2-NO₂ or 4-NO₂, similarly to CB1954 (Figures 3D and S2). T41L and T41F preferentially reduced 2-NO₂, and the double and triple mutants showed further improved regioselectivity. T41L/N71S/F124W displayed 100% regioselectivity in favor of the 2-hydroxylamine product (Figure 3F); that is, as the hydrophobicity of the substituent group increases (CH₃ < CH₃O < C₂H₄N), the preference for the adjacent nitro group increases. The changes in regioselectivity of the mutants were not accompanied by activity loss: T41L/N71S/F124W (the most active mutant) exhibited similar activity against 24DNT and a 4.4-fold increase in k_{cat}/K_m against 24DNAN (Table 1).

Molecular basis of regioselectivity of NfsB

Nitroreductase-catalyzed reduction occurs by a “ping-pong” mechanism: the prosthetic group FMN transfers a hydride from NAD(P)H to the adjacent nitro group of the bound substrate.^[10,22] The regioselectivity might therefore be determined by the binding orientation of the substrate: either a 2-NO₂ or 4-NO₂ group is positioned above N5 of reduced FMN, thereby leading to the corresponding 2-hydroxylamine or 4-hydroxylamine product.

The crystal structure of the T41L/N71S/F124W mutant was resolved to gain insight into how its active pocket is remodeled to accommodate substrates in different orientations for regioselective reduction of the 2-NO₂ group (Table 2). A comparison of the structures of T41L/N71S/F124W and wild-type NfsB showed no significant difference in overall structure (root mean square deviation 0.57 Å) but some conformational changes were observed in the active pocket (Figure 4A and B). The backbone conforma-

Table 1. Apparent steady-state kinetic parameters^[a,b] for the reduction of 24DNT and 24DNAN by wild-type NfsB and selected mutants.

NfsB/mutant	24DNT			24DNAN		
	$K_{m(\text{app})}$ [μM]	$k_{\text{cat}(\text{app})}$ [s^{-1}]	$k_{\text{cat}(\text{app})}/K_{m(\text{app})}$ [$\text{s}^{-1} \mu\text{M}^{-1}$]	$K_{m(\text{app})}$ [μM]	$k_{\text{cat}(\text{app})}$ [s^{-1}]	$k_{\text{cat}(\text{app})}/K_{m(\text{app})}$ [$\text{s}^{-1} \mu\text{M}^{-1}$]
wild-type	171.7 ± 1.4	23.15 ± 0.79	0.135	514.2 ± 40.1	9.33 ± 0.13	0.018
T41L	297.3 ± 5.0	31.40 ± 0.89	0.106	851.9 ± 75.1	18.01 ± 0.91	0.021
T41L/N71S	63.9 ± 5.6	5.32 ± 0.21	0.083	160.6 ± 13.3	8.35 ± 1.14	0.052
T41L/N71S/F124W	25.04 ± 0.36	2.95 ± 0.04	0.118	58.4 ± 6.7	4.61 ± 0.35	0.079

[a] Kinetic parameters were obtained by continuous monitoring of NADH consumption at 340 nm. All reactions used NADH (60 μM) as a co-substrate in Tris-HCl buffer (20 mM, pH 7.0) at 37 °C. The data were fitted to the Michaelis–Menten equation by nonlinear regression (Origin 8.5), and the errors were calculated from triplicates from the same enzyme preparation. [b] Calculated assuming two moles of NADH per mole of nitro group.^[22]

Table 2. X-ray data collection and model refinement statistics for T41L/N71S/F124W.

PDB ID	3X21	Refinement	
		no. reflections	48 630
Data collection		R_{work} (95% data)	0.210
space group	$P2_1$	R_{free} (5% data)	0.256
unit cell [\AA] <i>a</i>	95.410,	r.m.s.d. bond	
<i>b</i>	59.924,	distance [\AA]	0.007
<i>c</i>	220.063	r.m.s.d. bond	
β [°]	99.723	angle [°]	1.127
resolution [\AA]	50.00–3.00 (3.05–3.00)	Ramachandran plot	
		[% residues]	
no. observations	2 496 629	most-favored regions	94.6
no. unique	48 758(2405)	additional allowed	5.4
completeness [%]	99.4(99.9)	regions	
average $I/\sigma(I)$	9.869(6.206)	generously allowed	0
R_{merge} [%]	9.9(16.6)	regions	
		average B [\AA^2] no. non-H atoms	
		protein	52.3/16860
		water	49.1/6
		FMN	50.6/310

tion of L41 was identical to that of T41 (wild-type), but the leucine side chain was longer and in contact with W124, thus possibly leading to a more hydrophobic region above FMN. Moreover, the W124 ring was further from the isoalloxazine ring of FMN (relative to wild-type NfsB), thus allowing space for FMN to expand slightly. Although S71 was in a similar position to that of N71 (wild-type), the side chain of the adjacent residue (F70) had apparently rotated to be opposite the pocket, thus generating a wider entrance to the active site. These conformational changes (F70 and W124) might therefore reduce possible steric effects on substrate binding. The results suggest that the alteration in regioselectivity of T41L/N71S/F124W might be partly related to a hydrophobicity change and reduced steric effects, thereby enabling the 2-NO₂ group to be positioned close to the catalytic site.

To further understand the effects of these mutations on regioselectivity at the molecular level, we performed molecular docking simulations of 24DNT with T41L/N71S/F124W and the wild-type enzyme in AutoDock. This showed that the binding modes of 24DNT were different in the active pockets of the two enzymes, in good agreement with the experimental re-

sults. The wild-type NfsB allowed only one orientation of 24DNT, with the 4-NO₂ group pointing to N5 of FMN and the methyl group exposed to the solution (Figure 5). 24DNT assumed a different orientation with T41L/N71S/F124W, with 2-NO₂ close to the catalytic site and the methyl group bound in a hydrophobic region formed by the side chains of L41 and W124.

Analysis of the docking structures showed that 24DNT con-

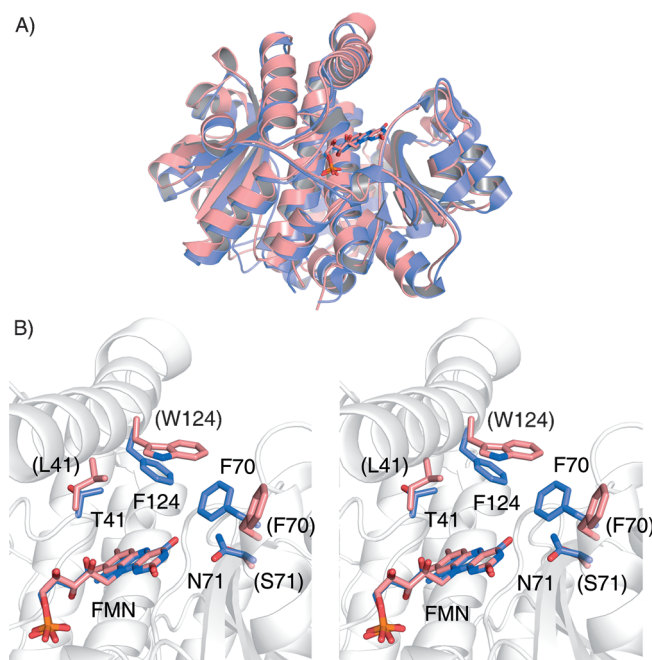


Figure 4. Structural comparison of wild-type NfsB and T41L/N71S/F124W mutant. Overlay of A) overall structures and B) active sites of wild-type NfsB (blue) and T41L/N71S/F124W mutant (pink). Bound FMN and residues at positions 41, 70, 71, and 124 are shown as sticks. Images were prepared with PyMOL version 1.5.0.4.^[23]

tacts the active site residues mainly by hydrophobic and π -stacking interactions (no hydrogen bonding). In both binding modes, 24DNT stacked above the FMN plane and was bound to the flavin by π - π stacking and nitro- π -stacking interactions. Although the stacking interactions were important for 24DNT binding, they were observed in two binding modes and might not explain the shift in regioselectivity. In addition to the stacking interactions with FMN, various other interactions with surrounding residues occurred. For the wild-type enzyme, the 4-NO₂ group was bound in a pocket containing T41, E165, G166, and F124, and was involved in nitro- π stacking interactions with F124, whereas the 2-NO₂ group and the methyl group were exposed to the solution (Figure 5A). For T41L/N71S/F124W, the methyl group was in hydrophobic contact with

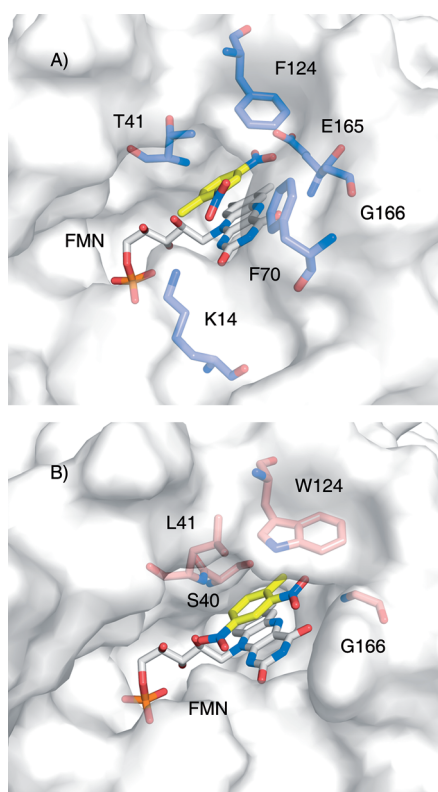


Figure 5. Molecular docking of 24DNT in the active sites of A) wild-type NfsB (residues involved in substrate binding shown in blue) and B) T41L/N71S/F124W mutant (pink). The substrate 24DNT (yellow) assumes different orientations in the two active pockets, thus leading to reduction of a 4-NO₂ group or a 2-NO₂ group. Bound FMN is shown as a stick model. Images were prepared with PyMOL version 1.5.0.4.^[23]

L41, G166, and W124, and the 2-NO₂ group was held by a nitro–indo interaction with W124 and positioned close to N5 of FMN to be reduced (Figure 5B). The hydrophobic interactions of L41 and W124 and/or the nitro–indo interaction of W124 might favor the binding mode of the 2-NO₂ group. In the crystal structure of the T41L/N71S/F124W mutant, the side chain of F70 (adjacent to S71) and the side chain of W124 had rotated away from the active pocket to create an open entrance; this might reduce steric hindrance of the 1-methyl group and favor its insertion. Residues 41, 71, and 124 exerted synergistic effects on the regioselectivity of NfsB.

The substrate substituents also affected regioselectivity. In contrast to the preference for the 4-NO₂ group of 24DNT, the wild-type NfsB reduced either of the two nitro groups of 24DNAN and CB1954. In the NfsB–CB1954 complex, the hydrophobic aziridinyl group was bound within the pocket, so its adjacent nitro group was close to the active site.^[10] Similarly, the docking results for 24DNAN show that the methoxy group was inserted into the pocket when the 2-NO₂ group was reduced (Figure S3). However, the methyl group of 24DNT was exposed to the solution and the 2-NO₂ group could not be reduced (Figure 5A). The binding modes of the three substrates suggest that the hydrophobic substituent groups might act as anchors to position the adjacent nitro group above N5 of FMN.

Conclusion

The regioselectivity of NfsB toward 24DNT was successfully shifted from the 4-NO₂ group to the 2-NO₂ group without loss of activity, by introducing three mutations: T41L, N71S, and F124W. The triple mutant displayed 100% regioselectivity for the 2-NO₂ group of 24DNAN. It is proposed that the side chains of L41, S71, and W124 enhance the hydrophobicity of the region above FMN and slightly change the shape of the catalytic pocket, thereby resulting in more favorable binding of 2-NO₂ than of 4-NO₂. This study investigated alterations in nitroreductase regioselectivity by structure-based engineering, and provides an example of a tailored enzyme for the reduction of a specific nitro group in a polynitroarene.

Experimental Section

Chemicals and reagents: NADH (Purity > 98%) was obtained from Sigma–Aldrich. 24DNT, 24DNAN, 2ANT, 4ANT and FMN were purchased from J&K (Beijing, China). Unless otherwise stated, other chemicals and reagents were of analytical grade. Chromatographic-grade methanol and acetonitrile were supplied by J&K (Beijing, China). Oligonucleotide primers were obtained from Takara (Dalian, China).

Cloning, expression, and purification of NfsB and its mutants: The *nfsB* gene (Gene ID: 945778) was amplified from *E. coli* K12 genomic DNA with primers *nfsBWTF* and *nfsBWTR* (Table S1) and cloned into pET28a (Novagen/Merck Millipore). Site-directed NfsB mutants were generated by overlap extension PCR and sequenced to confirm the amplification products. In brief, for each *nfsB* mutagenesis, two partially overlapping PCR products were generated by using the upstream primer *nfsBWTF* or downstream primer *nfsBWTR* with the corresponding internal primer (Table S1), and then annealed to create the full-length product, which was digested with Nde I and EcoR I restriction enzymes, ligated into pET28a, and then transformed into *E. coli* DH5 α for amplification. All mutants were confirmed by sequencing and then transformed into *E. coli* BL21(DE3) cells (Novagen) for expression as N-terminal His₆ enzymes.

A single colony was grown overnight and inoculated into LB medium supplemented with kanamycin. Nitroreductase expression was induced with isopropyl- β -thiogalactopyranoside (IPTG, 0.3 mM) at the early exponential phase (OD₆₀₀ = 0.5–0.6). The harvested cell pellet was suspended in sodium phosphate buffer (pH 7.4) containing NaCl (500 mM) and imidazole (20 mM), and lysed by high pressure homogenization at 4 °C. Recombinant nitroreductase was purified on a HiTrap chelating HP column (GE Healthcare) and buffer exchanged into Tris-HCl buffer (20 mM, pH 7.0) containing NaCl (50 mM) by using a PD-10 desalting column (GE Healthcare). For kinetic studies, the active fractions were incubated with pure FMN at 4 °C for at least 30 min before buffer exchange. The protein samples were more than 95% pure as estimated by SDS-PAGE, and their concentrations were determined by Bradford assays (BSA as the standard).

Products and regioselectivity of 24DNT and 24DNAN reduction: The products generated from the reduction of 24DNT and 24DNAN catalyzed by the nitroreductases were identified by reverse phase HPLC. The reaction mixture contained substrate (100 μ M), NADH (200 μ M), and enzyme (300 nM) in Tris-HCl buffer (20 mM, pH 7.0), and was incubated at 37 °C for 30 min in an anaerobic atmosphere

(Mitsubishi Anaeropack; Thermo Scientific) 30 min prior to and following the addition of nitroreductase. The reaction products were extracted with ethyl acetate and injected into a Hypersil C18 column (5 μm , 4.6 \times 250 mm; Thermo Scientific). For 24DNT, the reactants were injected into a column equilibrated with methanol/water (20:80), and eluted in isocratic mixture of methanol/water (50:50) over 15 min, followed by a 50–90% (v/v) methanol linear gradient over 10 min (flow rate 0.8 mL min⁻¹). For 24DNAN, the products were injected into a column equilibrated with acetonitrile/water (20:80), and eluted with a linear gradient of acetonitrile (40–80%, flow-rate 0.8 mL min⁻¹, monitored at 254 nm). The products of 24DNT and 24DNAN reduction were identified by HPLC-MS in an 1100 Series HPLC system (HewlettPackard) and a Finnigan TSQ 7000 triple quadrupole mass spectrometer. The mass spectrometer was equipped with an atmospheric pressure ionization (API) interface and an electrospray ion (ESI) source in positive or negative ion mode.

To distinguish the position of the hydroxylamino group, the reductive products of 24DNT and 24DNAN were chemically reduced to their corresponding amines, which were identified by comparison of their retention times. The hydroxylamino products were incubated for 15 min at 40 °C in freshly prepared potassium phosphate buffer (20 mM, pH 9.0) containing Na₂S (5 mM) and sodium thioglycolate (0.05%, w/v).^[24]

Steady-state kinetic studies: Nitroreductase activity toward 24DNT and 24DNAN for purified NfsB and its mutants was determined by monitoring the initial rate of oxidation of NADH at 340 nm. All assays were performed in Tris-HCl buffer (20 mM, pH 7.0) with NADH (60 μM) and substrate (varying concentrations), initiated by addition of purified enzymes (50 nM). The reaction temperature was 37 \pm 1 °C, and changes in absorbance were detected every 15 s for 5 min (during linearity). All reactions were replicated at least three times, and the data were fitted by non-linear regression (Origin 8.5 software; OriginLab, Northampton, MA).

Crystallization, data collection, and processing: Crystals of the T41L/N71S/F124W mutant (10 mg mL⁻¹) were grown in sodium acetate (100 mM, pH 4.6) containing poly(ethylene glycol) 3350 (16%, w/v; Sigma—Aldrich) and Tacsimate (pH 4.0, 2%, v/v; Hampton Research Corp.) at 4 °C by the hanging-drop vapor-diffusion method. Crystals, which appeared within two weeks, were rinsed in reservoir solution containing glycerol (25%, v/v) as a cryoprotectant for several seconds, and flash-frozen in liquid nitrogen. Diffraction data were collected at beamline BL-17U (Shanghai Synchrotron Radiation Facility, Shanghai, China) and processed using HKL2000.^[25] Full data collection statistics are listed in Table 2.

Structure determination and refinement: The structure of the T41L/N71S/F124W mutant was solved by molecular replacement with Phaser^[26] by using the structure of wild-type NfsB (PDB ID: 1DS7)^[18] as the starting structure. Further refinement and model adjustment were performed with PHENIX^[27] and Coot^[28] programs, respectively (structure-refinement statistics in Table 2). The coordinates and structure factors of the T41L/N71S/F124W mutant have been deposited in the Protein Data Bank (PDB ID: 3X21).

Molecular docking: To elucidate the molecular basis of the regioselectivity of the wild-type and T41L/N71S/F124W mutant, we docked 24DNT and 24DNAN to the active pockets of wild-type NfsB (PDB ID: 1DS7) and the T41L/N71S/F124W mutant (PDB ID: 3X21) in AutoDock 4.2.^[29] The GridBox parameters for docking the substrates to enzymes were determined (grid center coordinates: x = 2.103, y = -14.394, z = 0.138; size coordinates: x = 28, y = 28, z = 28). The docked structures were minimized by using a web

server (<http://lorenz.immstr.pasteur.fr/docking/index.php>). Substrate orientation and enzyme–substrate interactions were analyzed with PyMOL and LigPlot.^[23,30]

Acknowledgements

We would like to thank Dr. Tian Liu for valuable discussions and suggestions. This work was supported by China National Funds for Distinguished Young Scientists (31425021), the National High Technology Research and Development Program of China (2011AA10A204), National Natural Science Foundation of China (61202252), Specialized Research Fund for the Doctoral Program of Higher Education of China (P20120041120052), China Postdoctoral Science Foundation (2013M541214), Dalian Foundation of Science and Technology (2013E13SF114), The Fundamental Research Funds for the Central Universities (DUT13JB08), and Shanghai Key Lab of Chemical Biology (China).

Keywords: arylhydroxylamines • enzyme catalysis • nitroreductases • protein engineering • regioselectivity

- a) R. J. Knox, F. Friedlos, T. Marchbank, J. J. Roberts, *Biochem. Pharmacol.* **1991**, *42*, 1691–1697; b) D. G. Smith, A. D. Gribble, D. Haigh, R. J. Iffe, P. Lavery, P. Skett, B. P. Slingsby, R. Stacey, R. W. Ward, A. West, *Bioorg. Med. Chem. Lett.* **1999**, *9*, 3137–3142; c) P. M. Vyas, S. Roychowdhury, P. M. Woster, C. K. Svensson, *Biochem. Pharmacol.* **2005**, *70*, 275–286; d) J. S. Yadav, B. V. S. Reddy, P. Sreedhar, *Adv. Synth. Catal.* **2003**, *345*, 564–567.
- a) C.-M. Ho, T.-C. Lau, *New J. Chem.* **2000**, *24*, 859–863; b) J. D. Spence, A. E. Raymond, D. E. Norton, *Tetrahedron Lett.* **2003**, *44*, 849–851; c) H. Takeuchi, J.-i. Tateiwa, S. Hata, K. Tsutsumi, Y. Osaki, *Eur. J. Org. Chem.* **2003**, 3920–3922; d) V. Sridharan, K. Karthikeyan, S. Muthusubramanian, *Tetrahedron Lett.* **2006**, *47*, 4221–4223; e) A. A. Lamar, K. M. Nicholas, *Tetrahedron* **2009**, *65*, 3829–3833; f) Y. Wang, L. Ye, L. Zhang, *Chem. Commun.* **2011**, *47*, 7815–7817; g) R. S. Srivastava, K. M. Nicholas, *J. Am. Chem. Soc.* **1997**, *119*, 3302–3310.
- a) S. Ung, A. Falguières, A. Guy, C. Ferroud, *Tetrahedron Lett.* **2005**, *46*, 5913–5917; b) Q. X. Shi, R. W. Lu, K. Jin, Z. X. Zhang, D. F. Zhao, *Chem. Lett.* **2006**, *35*, 226–227; c) A. B. Gamble, J. Garner, C. P. Gordon, S. M. J. O’Conner, P. A. Keller, *Synth. Commun.* **2007**, *37*, 2777–2786; d) S. Liu, Y. Wang, J. Jiang, Z. Jin, *Green Chem.* **2009**, *11*, 1397–1400; e) S. Liu, Y. Wang, X. Yang, J. Jiang, *Res. Chem. Intermed.* **2012**, *38*, 2471–2478; f) M. Bartra, P. Romea, F. Urpí, J. Vilarrasa, *Tetrahedron* **1990**, *46*, 587–594.
- a) Y. Takenaka, T. Kiyosu, J.-C. Choi, T. Sakakura, H. Yasuda, *Green Chem.* **2009**, *11*, 1385–1390; b) Z. Rong, W. Du, Y. Wang, L. Lu, *Chem. Commun.* **2010**, *46*, 1559–1561; c) A. K. Shil, P. Das, *Green Chem.* **2013**, *15*, 3421–3428.
- a) G. Neri, G. Rizzo, C. Milone, S. Galvagno, M. G. Musolino, G. Capanneli, *Appl. Catal. A* **2003**, *249*, 303–311; b) Y. Takenaka, T. Kiyosu, G. Mori, J.-C. Choi, T. Sakakura, H. Yasuda, *Catal. Today* **2011**, *164*, 580–584; c) D. Beaudoin, J. D. Wuest, *Tetrahedron Lett.* **2011**, *52*, 2221–2223; d) Y. Takenaka, T. Kiyosu, J.-C. Choi, T. Sakakura, H. Yasuda, *ChemSusChem* **2010**, *3*, 1166–1168.
- F. Li, J. Cui, X. Qian, R. Zhang, *Chem. Commun.* **2004**, 2338–2339.
- F. Li, J. Cui, X. Qian, R. Zhang, Y. Xiao, *Chem. Commun.* **2005**, 1901–1903.
- H.-H. Nguyen-Tran, G.-W. Zheng, X.-H. Qian, J.-H. Xu, *Chem. Commun.* **2014**, *50*, 2861–2864.
- S. O. Vass, D. Jarrom, W. R. Wilson, E. I. Hyde, P. F. Searle, *Br. J. Cancer* **2009**, *100*, 1903–1911.
- E. Johansson, G. N. Parkinson, W. A. Denny, S. Neidle, *J. Med. Chem.* **2003**, *46*, 4009–4020.
- G. A. Prosser, J. N. Copp, S. P. Syddall, E. M. Williams, J. B. Smaill, W. R. Wilson, A. V. Patterson, D. F. Ackerley, *Biochem. Pharmacol.* **2010**, *79*, 678–687.

- [12] G. M. Anlezark, T. Vaughan, E. Fashola-Stone, N. P. Michael, H. Murdoch, M. A. Sims, S. Stubbs, S. Wigley, N. P. Minton, *Microbiology* **2002**, *148*, 297–306.
- [13] C. D. Emptage, R. J. Knox, M. J. Danson, D. W. Hough, *Biochem. Pharmacol.* **2009**, *77*, 21–29.
- [14] H. Guillén, J. A. Curiel, J. M. Landete, R. Muñoz, T. Herraiz, *J. Agric. Food Chem.* **2009**, *57*, 10457–10465.
- [15] D. Jarrom, M. Jaberipour, C. P. Guise, S. Daff II, S. A. White, P. F. Searle, E. I. Hyde, *Biochemistry* **2009**, *48*, 7665–7672.
- [16] P. R. Race, A. L. Lovering, S. A. White, J. I. Grove, P. F. Searle, C. W. Wrighton, E. I. Hyde, *J. Mol. Biol.* **2007**, *368*, 481–492.
- [17] A. L. Lovering, E. I. Hyde, P. F. Searle, S. A. White, *J. Mol. Biol.* **2001**, *309*, 203–213.
- [18] G. N. Parkinson, J. V. Skelly, S. Neidle, *J. Med. Chem.* **2000**, *43*, 3624–3631.
- [19] S. Zenno, H. Koike, M. Tanokura, K. Saigo, *J. Biochem.* **1996**, *120*, 736–744.
- [20] a) J. I. Grove, A. L. Lovering, C. Guise, P. R. Race, C. J. Wrighton, S. A. White, E. I. Hyde, P. F. Searle, *Cancer Res.* **2003**, *63*, 5532–5537; b) S.-W. LinWu, C.-A. Wu, F.-C. Peng, A. H.-J. Wang, *Biochem. Pharmacol.* **2012**, *83*, 1690–1699.
- [21] M. T. Reetz, J. D. Carballeira, *Nat. Protoc.* **2007**, *2*, 891–903.
- [22] P. R. Race, A. L. Lovering, R. M. Green, A. Ossor, S. A. White, P. F. Searle, C. J. Wrighton, E. I. Hyde, *J. Biol. Chem.* **2005**, *280*, 13256–13264.
- [23] <http://www.pymol.org>.
- [24] P. D. Fiorella, J. C. Spain, *Appl. Environ. Microbiol.* **1997**, *63*, 2007–2015.
- [25] Z. Otwinowski, W. Minor, *Methods Enzymol.* **1997**, *276*, 307–326.
- [26] A. J. McCoy, R. W. Grosse-Kunstleve, P. D. Adams, M. D. Winn, L. C. Storoni, R. J. Read, *J. Appl. Crystallogr.* **2007**, *40*, 658–674.
- [27] P. D. Adams, P. V. Afonine, G. Bunkóczi, V. B. Chen, I. W. Davis, N. Echols, J. J. Headd, L.-W. Hung, G. J. Kapral, R. W. Grosse-Kunstleve, A. J. McCoy, N. W. Moriarty, R. Oeffner, R. J. Read, D. C. Richardson, J. S. Richardson, T. C. Terwilliger, P. H. Zwart, *Acta Crystallogr. Sect. D* **2010**, *66*, 213–221.
- [28] P. Emsley, K. Cowtan, *Acta Crystallogr. Sect. D* **2004**, *60*, 2126–2132.
- [29] G. M. Morris, R. Huey, W. Lindstrom, M. F. Sanner, R. K. Belew, D. S. Goodsell, A. J. Olson, *J. Comput. Chem.* **2009**, *30*, 2785–2791.
- [30] A. C. Wallace, R. A. Laskowski, J. M. Thornton, *Protein Eng.* **1995**, *8*, 127–134.

Manuscript received: February 9, 2015

Final article published: April 27, 2015